RMetS
Royal Meteorological Society

Analytical expressions for entrainment and detrainment in cumulus convection

Wim C. de Rooy[a]* and A. Pier Siebesma[a,b]
[a]*Royal Netherlands Meteorological Institute (KNMI), De Bilt, The Netherlands*
[b]*Department of Multi-Scale Physics, Delft University of Technology, The Netherlands*
*Correspondence to: Wim de Rooy, Royal Netherlands Meteorological Institute (KNMI), PO Box 201, 3730 AE De Bilt, The Netherlands. E-mail: rooyde@knmi.nl

Analytical expressions for entrainment and detrainment are derived based on general total water specific humidity and mass budget equations. From these expressions, containing a small-scale turbulent and a larger-scale organized term, a physical picture emerges for a shallow cumulus cloud ensemble in which the individual clouds have a massive entrainment at the bottom, lateral turbulent mixing with constant mass flux between bottom and top, and massive detrainment at the top. Combining these results with the general budget equation for vertical velocity, new formulae for entrainment and detrainment rates can be expressed in terms of buoyancy, vertical velocity and cloud fraction. For a variety of shallow convection cases, results from large-eddy simulations show a good correspondence of these new formulae with more traditional methods to diagnose entrainment and detrainment rates. Moreover, the formulae give insight into the behaviour and the physical nature of the mixing coefficients. They explain the observed large variability of the detrainment. The formulae cannot be directly applied as a parametrization. However, it is demonstrated how they can be used to evaluate existing parametrization approaches and as a sound physical base for future parametrization developments.
Copyright © 2010 Royal Meteorological Society

Key Words: lateral mixing; mass flux; large-eddy simulation; cloud ensemble

Received 5 August 2009; Revised 16 April 2010; Accepted 20 April 2010; Published online in Wiley InterScience 14 July 2010

Citation: de Rooy WC, Pier Siebesma A. 2010. Analytical expressions for entrainment and detrainment in cumulus convection. *Q. J. R. Meteorol. Soc.* **136**: 1216–1227. DOI:10.1002/qj.640

1. Introduction

Lateral mixing between convective clouds and their environment represented by entrainment and detrainment are key processes in atmospheric moist convection and the uncertainty of its strength is still a main source in climate model uncertainty (Murphy *et al.*, 2004; Rougier *et al.*, 2009). The strong positive impact of new entrainment and detrainment representation on the predictive skill of numerical weather prediction (NWP) models (Bechtold *et al.*, 2008) shows both the importance and the relative infancy of our knowledge of these processes.

The concept and relevance of entrainment of environmental quiescent air into convective cumulus updraughts was first pointed out by Stommel (1947) and were followed by numerous observational studies of cumulus clouds with aircrafts (e.g. Warner, 1955). In these studies entrainment strength could be determined through the ratio between the measured liquid water in clouds and its adiabatic value. The first quantitative descriptions of entrainment originated from laboratory experiments of thermal plumes (Morton *et al.*, 1956; Turner, 1963) describing an increasing mass flux M with height

$$\frac{1}{M}\frac{\partial M}{\partial z} = \epsilon \simeq \frac{0.2}{R}, \tag{1}$$

where R is the radius of the rising plume and ϵ is the fractional entrainment coefficient. Many of the early cloud models have adopted this entraining plume model. A distinction

Copyright © 2010 Royal Meteorological Society

between entrainment due to turbulent mixing at the cloud edge and organized inflow of environmental air induced by the increase of the vertical velocity due to buoyancy was first pointed out by Houghton and Cramer (1951) and its relevance has been recently re-emphasized by Holloway and Neelin (2009)

$$\frac{1}{M}\frac{\partial M}{\partial z} = \epsilon_{\mathrm{dyn}} + \epsilon_{\mathrm{turb}}\,. \tag{2}$$

Since the dynamical (organized) and turbulent fractional entrainment rates are by definition positive, they cause the mass flux to increase with height. This is in agreement with dry plumes where entrained air from the environment becomes part of the plume after the mixing process. However, cloudy updraughts can actually also exhibit a decreasing mass flux with height, for instance due to mixing of dry environmental air. The evaporative cooling can actually reduce the updraught area and/or the updraught velocity so that the mass flux can also decrease with height. This so-called detrainment process is, in many respects, the mirror image of entrainment and can also be subdivided into a dynamical and a turbulent part:

$$\frac{1}{M}\frac{\partial M}{\partial z} = \epsilon_{\mathrm{dyn}} + \epsilon_{\mathrm{turb}} - \delta_{\mathrm{dyn}} - \delta_{\mathrm{turb}}\,. \tag{3}$$

Mass flux parametrizations of cumulus convection in NWP and climate models have to take into account the effect of a whole ensemble of clouds rather than a single cloud element. With the exception of the seminal work of Arakawa and Schubert (1974), most mass flux parametrizations employ a so-called bulk approach in which all active cloud elements are represented in one steady-state updraught representing the whole cloud ensemble.

Numerous entrainment and detrainment parametrizations have been proposed for such mass flux bulk schemes. Popular formulations proposed by Tiedtke (1989), Bechtold *et al.* (2008), Nordeng (1994) and Gregory and Rowntree (1990) can be ordered in terms of the right-hand side of (3). Tiedtke (1989) and Nordeng (1994) assume that ϵ_{turb} and δ_{turb} are equal and given by (1), while in Bechtold *et al.* (2008) ϵ_{turb} depends on the saturation specific humidity. Gregory and Rowntree (1990) also propose (1) for ϵ_{turb} but utilize a systematic smaller δ_{turb}. Dynamical entrainment ϵ_{dyn} is based on moisture convergence in Tiedtke (1989), on momentum convergence in Nordeng (1994), on relative humidity in Bechtold *et al.* (2008), and absent in Gregory and Rowntree (1990). Organized detrainment is in general formulated as a massive lateral outflow of mass around the neutral buoyancy level although the precise details differ in the cited parametrizations. In the above-cited parametrizations typically a fixed value of $R \simeq 500$ m for shallow clouds and $R \simeq 2000$ m for deep convection is used.

Another class of entrainment/detrainment parametrizations, that does not distinguish between dynamical and turbulent mixing, is based on the 'buoyancy sorting' concept introduced by Raymond and Blyth (1986). This buoyancy sorting concept is transformed into a operational parametrization by Kain and Fritsch (1990). In Kain and Fritsch (1990) an ensemble of mixtures of cloudy and environmental air is formed, where each ensemble member has a different concentration of environmental air. If resulting mixtures are positively buoyant, they remain in the updraught and are part of the entrainment process while negatively buoyant mixtures are rejected from the updraught and are part of the detrainment process. A number of recently proposed shallow cumulus convection schemes (Bretherton *et al.*, 2004; de Rooy and Siebesma, 2008; Neggers *et al.*, 2009) are based on this buoyancy sorting concept. Finally a large number of parametrizations for ϵ and (sometimes) δ have been published that are directly or indirectly inspired on large-eddy simulation (LES) results of shallow cumulus convection (e.g. Siebesma, 1998; Grant and Brown, 1999; Neggers *et al.*, 2002; Gregory *et al.*, 2000; Lappen and Randall, 2001).

The objectives of this paper are twofold. Firstly, to create some order in all the proposed parametrizations, general expressions for the dynamical and turbulent entrainment and detrainment rates will be derived. Based on these expressions, a physical picture emerges that resembles Arakawa and Schubert (1974) and Nordeng (1994). Furthermore, through combining budget equations of mass, total water specific humidity and vertical velocity, we will derive analytical expressions for ϵ and δ that can be evaluated using LES. The latter expressions show that the entrainment formulations proposed by Nordeng (1994) and Gregory (2001) can be viewed as special cases. The analytical expressions for ϵ and δ cannot be used directly as parametrizations as no closure assumptions have been imposed. Secondly, in section 3 we use LES results for different shallow cumulus cases to critically evaluate these analytical expressions. With the help of the expressions, different aspects of ϵ and δ can be explained, e.g. the large variability of the detrainment coefficient. Moreover, the expressions are used to evaluate existing parametrization approaches and it is demonstrated how they can serve as a sound physical base for future parametrization developments.

2. Derivation of the lateral mixing expressions

2.1. Basics

A convenient starting point is the conservation law for an arbitrary variable ϕ:

$$\frac{\partial \phi}{\partial t} + \boldsymbol{\nabla}\cdot\mathbf{v}\phi = F\,, \tag{4}$$

where $\mathbf{v}$ denotes the three-dimensional velocity vector and where all possible sources and sinks of ϕ are collected in F. For the sake of simplicity, we assume a Boussinesq flow, implying that the density in (4) is constant. We consider a domain with a horizontal area A and we are interested in the lateral mixing between a cloudy area A_{c} and a complementary environmental area A_{e} at a given height z, such as sketched schematically in Figure 1. At this point we do not need to be more specific on the precise definition of cloudy area, but it should be noted that it may consist of many different 'blobs' (or clouds) that can change in shape and size as a function of time and height.

By integrating (4) horizontally over the cloudy area $A_{\mathrm{c}}(z,t)$ and applying Leibniz integral rule and Gauss divergence theorem, a transparent conservation equation

Copyright © 2010 Royal Meteorological Society

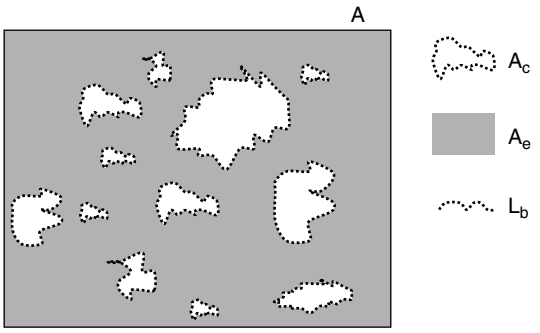

Figure 1. Schematic diagram showing an ensemble of clouds at a certain height. A, A_c, and A_e represent the total horizontal domain area ($A_c + A_e$), the cloudy area (white), and the environmental area (grey), respectively. The interface between the cloudy area and the environment is plotted as a dashed line and has a total length L_b.

of the cloudy area for ϕ can be deduced (Siebesma, 1998):

$$\frac{\partial a_c \phi_c}{\partial t} + \frac{1}{A}\oint_{\text{interface}} \widehat{\mathbf{n}} \cdot (\mathbf{u} - \mathbf{u}_i)\, \phi \, dl + \frac{\partial a_c \overline{w\phi}^c}{\partial z} = a_c F_c \,, \tag{5}$$

where $a_c = A_c/A$ is the fractional cloud cover, $\widehat{\mathbf{n}}$ is an outward-pointing unit vector perpendicular to the interface, $\mathbf{u}$ is the full 3D velocity vector at the interface, $\mathbf{u}_i$ is the velocity of the interface and w is the vertical component of the velocity field. Overbars and variables annotated with c denote averages over the cloudy part, i.e.

$$\overline{\phi}^c \equiv \phi_c \equiv \frac{1}{A_c}\iint_{\text{cloudy area}} \phi \, dx dy \,. \tag{6}$$

In the special case $\phi = 1$ and $F_c = 0$, we recover the continuity equation

$$\frac{\partial a_c}{\partial t} + \frac{1}{A}\oint_{\text{interface}} \widehat{\mathbf{n}} \cdot (\mathbf{u} - \mathbf{u}_i)\, dl + \frac{\partial a_c w_c}{\partial z} = 0 \,. \tag{7}$$

As we are interested in the fluxes over the cloud boundary, we also define averages over the interface as

$$\overline{u}^b \equiv u_b \equiv \frac{1}{L_b}\oint_{\text{interface}} \widehat{\mathbf{n}} \cdot (\mathbf{u} - \mathbf{u}_i)\, dl \,, \tag{8}$$

$$\overline{\phi}^b \equiv \phi_b \equiv \frac{1}{L_b}\oint_{\text{interface}} \phi \, dl \,, \tag{9}$$

where u_b is the net mean velocity through the cloud boundaries, ϕ_b is the mean of property ϕ along the cloud boundaries, and L_b is the total length of the interface. For both the interface and the cloudy area, we employ a decomposition of the fluxes into a mean and a fluctuating part:

$$\overline{u\phi}^b \equiv u_b \phi_b + \overline{u'\phi'}^b \,, \tag{10}$$

$$\overline{w\phi}^c \equiv w_c \phi_c + \overline{w'\phi'}^c \,, \tag{11}$$

where the primes denote deviations with respect to the cloudy part or the interface dependent on the used average.

The advantage of the decomposition of the flux on the interface is that it provides a natural distinction between the small-scale diffusive, turbulent mixing ($\overline{u'\phi'}^b$) and advective transport caused by organized motions across the interface ($u_b \phi_b$).

We assume that A is large enough to contain a large cumulus ensemble, so that Eqs. 5 and 7 can be assumed to be time-independent (Siebesma and Cuijpers, 1995). The resulting stationary form of Eqs. 5 and 7, together with Eqs. 8, 9, 10 and 11 can be written as

$$\frac{L_b}{A_c}\left(\overline{u'\phi'}^b + u_b \phi_b\right) + \frac{1}{a_c}\frac{\partial a_c w_c \phi_c}{\partial z} + \frac{1}{a_c}\frac{\partial a_c \overline{w'\phi'}^c}{\partial z} = F_c \,, \tag{12}$$

$$\frac{L_b u_b}{A_c} + \frac{1}{a_c}\frac{\partial a_c w_c}{\partial z} = 0 \,. \tag{13}$$

In most previous theoretical studies on cumulus clouds and lateral mixing (e.g. Asai and Kasahara, 1967; Randall and Huffman, 1982; Cotton, 1975), it has been assumed that the cloud fraction does not change with height. In that case there is a direct relationship between u_b and the divergence of the vertical velocity field. While constant cloud fraction might be a reasonable assumption for individual clouds, we will release this restriction in the present case where we are interested in the lateral mixing process between a whole shallow cumulus ensemble and its environment. In that case many LES studies showed that the cloud fraction varies strongly with height (e.g. Siebesma and Cuijpers, 1995; Stevens *et al.*, 2001; Brown *et al.*, 2002).

The turbulent flux across the cloud interface can be well approximated by an eddy diffusivity approach (Asai and Kasahara, 1967; Kuo, 1962):

$$\begin{aligned} \overline{u'\phi'}^b &\simeq K(\ell)\frac{(\phi_c - \phi_e)}{\ell} \\ &\simeq \eta \ell \mid \Delta w(\ell) \mid \frac{(\phi_c - \phi_e)}{\ell} \\ &\simeq \eta \mid w_c \mid (\phi_c - \phi_e) \,. \end{aligned} \tag{14}$$

In the first step, the horizontal gradient of the field ϕ is evaluated at a scale ℓ which is of the order of the typical radius of a cloudy updraught. The eddy diffusivity K in the second step is expressed as the product of a length-scale, a velocity difference over that length-scale and a dimensionless constant η . Obviously we have taken the same length-scale that is used to estimate the horizontal gradient. In the last step, we used the fact that the vertical velocity in the environment is much smaller than in the cloud. From here on, the modulo signs for w_c are omitted because we only consider updraughts.

For the advective transport term across the interface, $u_b \phi_b$, we use, following Asai and Kasahara (1967), an upwind approximation

$$\phi_b = \phi_c \text{ if } u_b > 0, \;\; \partial M/\partial z < 0 \text{ (divergence)}, \tag{15}$$

$$\phi_b = \phi_e \text{ if } u_b < 0, \;\; \partial M/\partial z > 0 \text{ (convergence)}. \tag{16}$$

Note that the sign of u_b is directly determined by the vertical gradient of the mass flux $M \equiv a_c w_c$ (13). Using

Copyright © 2010 Royal Meteorological Society

(14), (15), and (16) in (12) and eliminating the interface velocity u_b by using the continuity equation 13 finally gives

$$H(-u_\mathrm{b})\left(\frac{1}{a_\mathrm{c}}\frac{\partial a_\mathrm{c} w_\mathrm{c}}{\partial z}\right)(\phi_\mathrm{c}-\phi_\mathrm{e})+\frac{L_\mathrm{b}}{A_\mathrm{c}}\eta\, w_\mathrm{c}(\phi_\mathrm{c}-\phi_\mathrm{e}) + w_\mathrm{c}\frac{\partial \phi_\mathrm{c}}{\partial z}+\frac{1}{a_\mathrm{c}}\frac{\partial a_\mathrm{c}\overline{w'\phi'}^{\mathrm{c}}}{\partial z}=F_\mathrm{c}\,, \tag{17}$$

where H denotes the Heaviside function. The first term in (17) represents the organized transport across the cloud interface. Note that this term only has a non-zero contribution in the case of convergence. In the case of divergence, the organized term will show up in the equation for the environment which will not be considered in this paper. The second term represents the turbulent lateral mixing, the third term the vertical advection and the fourth term represents the subplume contributions to the vertical transport.

2.2. Budget equation for moist conserved variables

So far we have not specified ϕ. For the ultimate expressions for entrainment and detrainment we will need budget equations for w_c (section 2.3) and a moist conserved variable. The cloudy area is often defined in such a way that the contribution of the subplume vertical fluxes of moist conserved variables is minimized (Siebesma and Cuijpers, 1995). In the validation section, we will use a definition for the cloudy area as that part of the horizontal domain A that contains non-zero amounts of condensed water and that is also positively buoyant, known as the cloud core sampling method (e.g. Siebesma and Cuijpers, 1995). This latter condition is added to make sure that passive cloud elements that do not contribute to the vertical transport are excluded. With such a definition, the subplume covariance contribution for a moist conserved variable can usually be ignored (Siebesma and Cuijpers, 1995). Furthermore, for moist conserved variables such as the total water specific humidity q_t, there are in the absence of precipitation no sources and sinks, i.e. $F_{\mathrm{c},q_\mathrm{t}}=0$. For (heavy) precipitating convection $F_{\mathrm{c},q_\mathrm{t}}$ should be taken into account, but here we will only investigate (almost) non-precipitating shallow convection cases. Ignoring the source/sink and the subplume term allows us to rewrite (17) with $\phi = q_\mathrm{t}$ in a more familiar form:

$$\frac{\partial q_{\mathrm{t,c}}}{\partial z}=-\left\{H(-u_\mathrm{b})\left(\frac{1}{M}\frac{\partial M}{\partial z}\right)+\eta\,\frac{L_\mathrm{b}}{A_\mathrm{c}}\right\}(q_{\mathrm{t,c}}-q_{\mathrm{t,e}})\,, \tag{18}$$

where we recognize the entraining plume form of Betts (1975):

$$\frac{\partial q_{\mathrm{t,c}}}{\partial z}=-\epsilon_{q\mathrm{t}}(q_{\mathrm{t,c}}-q_{\mathrm{t,e}})\,, \tag{19}$$

in which the so-called fractional entrainment rate ϵ appears. Note that thus far we have not introduced ϵ in our derivation. This is in contrast with other studies (e.g. Gregory, 2001) where ϵ is already introduced at an earlier stage. Here we accept (19) as the definition of the fractional lateral entrainment ϵ because this equation describes how ϵ is used in parametrization schemes as well as how ϵ is diagnosed from LES. Taking (19) as the definition of ϵ allows us to write the following expression for the entrainment based on the budget equation 18 for q_t:

$$\epsilon=\epsilon_\mathrm{turb}+\epsilon_\mathrm{dyn}=\frac{\eta L_\mathrm{b}}{A_\mathrm{c}}+H(-u_\mathrm{b})\frac{1}{M}\frac{\partial M}{\partial z}\,, \tag{20}$$

where we made an explicit distinction between turbulent, ϵ_turb, and dynamical, ϵ_dyn, entrainment as introduced by Houghton and Cramer (1951). It is natural to identify the first term on the RHS of (20) with ϵ_turb and the second term on the RHS with ϵ_dyn. Likewise we can derive an expression for the fractional detrainment rate if we rewrite the steady state continuity equation 13 in a more familiar form:

$$\frac{1}{M}\frac{\partial M}{\partial z}=(\epsilon-\delta)\,, \tag{21}$$

and use this simply as a definition of the fractional detrainment rate δ. In that case we find a similar expression for δ:

$$\delta=\delta_\mathrm{turb}+\delta_\mathrm{dyn}=\frac{\eta L_\mathrm{b}}{A_\mathrm{c}}-H(u_\mathrm{b})\frac{1}{M}\frac{\partial M}{\partial z}\,. \tag{22}$$

Again it is natural to identify the first term on the RHS of (22) with δ_turb and the second term on the RHS with δ_dyn.

So for divergent conditions ($u_\mathrm{b}>0$ or $\partial M/\partial z<0$) $\epsilon_\mathrm{dyn}=0$, whereas for convergent conditions ($u_\mathrm{b}<0$ or $\partial M/\partial z>0$) $\delta_\mathrm{dyn}=0$. In shallow convection cases, the mass flux in the cloud layer will usually decrease (e.g. Siebesma and Cuijpers, 1995; de Rooy and Siebesma, 2008). Consequently, Eqs. 20 and 22 suggest a picture in line with Arakawa and Schubert (1974) and Nordeng (1994) of an ensemble of clouds where every individual cloud has a massive entrainment at the bottom, lateral turbulent mixing with constant mass flux in the cloud between bottom and top, and massive detrainment at the top (Figure 2). As a result of different cloud sizes in the ensemble, the massive detrainment of the various clouds shows up as a dynamical detrainment term. Different from Arakawa and Schubert (1974) is the appearance of a detrainment term in the turbulent lateral mixing, δ_turb. Figure 2 reveals that it is only the massive detrainment that regulates the shape of the cloud layer mass flux profile and consequently determines primarily where the updraught properties are deposited in the environment. This picture is consistent with de Rooy and Siebesma (2008) who use only the detrainment to describe variations in the shape of the shallow convection mass flux profile.

2.3. Budget equation for vertical velocity

For the vertical velocity equation, there are sinks and sources due to buoyancy and pressure perturbations

$$F_\mathrm{c,w}=B-\overline{\frac{\partial p'}{\partial z}}^{\mathrm{c}} \tag{23}$$

with

$$B=g\frac{\theta_{v,\mathrm{c}}-\overline{\theta_v}}{\overline{\theta_v}}\,, \tag{24}$$

where B is the buoyancy, p' in the second term on the RHS of (23) refers to pressure fluctuations with respect to the hydrostatic pressure, g is the acceleration due to gravity,

Copyright © 2010 Royal Meteorological Society

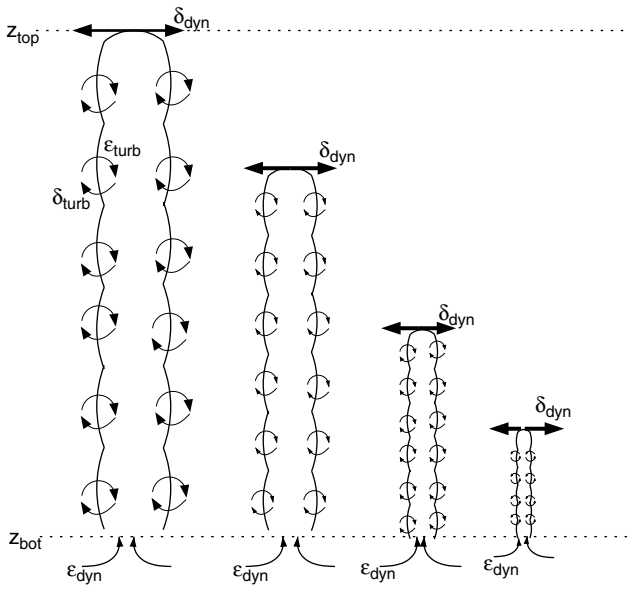

Figure 2. Schematic diagram of a cloud ensemble with massive entrainment, $\epsilon_{\rm dyn}$, at cloud base ($z_{\rm bot}$) and massive detrainment, $\delta_{\rm dyn}$, at the top of individual clouds. From cloud base to the top of individual clouds, turbulent lateral mixing takes place, presented by $\epsilon_{\rm turb}$ and $\delta_{\rm turb}$. For individual clouds the mass flux is constant with height. The deepest cloud reaches height $z_{\rm top}$, the top of the cloud layer. This picture is valid for divergent conditions, i.e. $\partial M/\partial z < 0$, which is usually the case for shallow convection.

and θ_v is the virtual potential temperature. As already mentioned by List and Lozowski (1970) and Holton (1973), the inclusion of the pressure pertubation term (second term on the RHS of (23)) can be important, certainly for heavy precipitating cumulus. Most recent studies, but in contrast to our approach, consider the effect of the pressure perturbation term within the context of a simplified vertical velocity equation, in which ϵ is already introduced. In some studies (e.g. Siebesma *et al.*, 2003) the pressure perturbation term was then scaled with the entrainment term and sometimes with the buoyancy term as well (Bretherton *et al.*, 2004). Uncommon was the approach of Gregory (2001), who used the detrainment coefficient to scale the pressure perturbation term. However, in the original work of Simpson and Wiggert (1969), and based on the work of Turner (1963), the effect of pressure perturbations was taken into account with a virtual mass coefficient which reduced the buoyancy term.

Another approximation we have to make concerns the subplume (variance) term in the budget equation 17 for $w_{\rm c}$. In contrast to the budget equation for $q_{\rm t}$, the subplume term cannot be ignored for vertical velocity. Recently, sophisticated parametrizations have been developed within a mass flux framework (Lappen and Randall, 2001) to represent these subplume-scale fluxes. In a more simple and often applied approach, the effect of this subplume turbulence term is scaled with the buoyancy and taken into account by a buoyancy reduction factor, α (e.g. Simpson and Wiggert, 1969; Gregory, 2001; Siebesma *et al.*, 2003). Formally the scaling of both the subplume term for vertical velocity and the pressure fluctuation term with the buoyancy can be written as

$$B - \overline{\frac{\partial p'}{\partial z}}^{\rm c} - \frac{1}{a_{\rm c}}\frac{\partial a_{\rm c}\overline{w'w'}^{\rm c}}{\partial z} \approx \alpha B\,. \qquad (25)$$

Preferably an adequate scaling of the pressure perturbation and subplume variance term should be determined from directly diagnosed vertical velocity budget terms in LES for different shallow convection cases. Such LES experiments are outside the scope of this paper, but recent LES results (Voogd, 2009) addressing exactly this problem support the scaling of both the subplume and the pressure perturbation term with the buoyancy (as in Simpson and Wiggert, 1969, and (25)) using an optimal reduction factor α of ≈ 0.6. Note that, based on laboratory experiments, Simpson and Wiggert (1969) found a similar value for α, namely 2/3. Because the choice of a proper α is important, we will return to this issue in the results section.

If we apply the above-mentioned assumptions for the forcing terms and subplume turbulence and taking the usual approximation in mass flux schemes $w_{\rm e} << w_{\rm c}$, (17) with $\phi = w$ results in the following vertical velocity equation:

$$H(-u_{\rm b})\left(\frac{1}{M}\frac{\partial M}{\partial z}\right) + \eta\frac{L_{\rm b}}{A_{\rm c}} = \frac{\alpha B}{w_{\rm c}^2} - \frac{1}{w_{\rm c}}\frac{\partial w_c}{\partial z}\,. \qquad (26)$$

2.4. *Analytical expressions for entrainment and detrainment*

A direct comparison of (26) with (18) allows new expressions of ϵ and δ in terms of buoyancy, vertical velocity and cloud fraction:

$$\epsilon_w = \frac{\alpha B}{w_{\rm c}^2} - \frac{1}{w_{\rm c}}\frac{\partial w_{\rm c}}{\partial z}\,, \qquad (27)$$

$$\delta_w = \frac{\alpha B}{w_{\rm c}^2} - \frac{2}{w_{\rm c}}\frac{\partial w_c}{\partial z} - \frac{1}{a_{\rm c}}\frac{\partial a_c}{\partial z}\,, \qquad (28)$$

where subscript w is used to distinguish these expressions from ϵ diagnosed using (19), denoted as ϵ_{qt}, and δ diagnosed from (21) and (19), denoted as δ_{qt}. So by using (26) we have eliminated the net exchange coefficient, η, as well as the Heaviside function in front of the dynamical mixing terms. As a consequence of the latter elimination, the analytical expressions (27) and (28) are now valid for both divergent and convergent conditions. Note that (27) and (28) cannot be used (directly) as a parametrization because $w_{\rm c}$ and the buoyancy themselves depend on ϵ, nor is it straightforward to approximate $(1/a_{\rm c})\partial a_{\rm c} z$. Validation of the expressions (27) and (28) as well as a discussion on the behaviour of the separate terms will be presented in the validation section.

3. Analysis and validation with LES

3.1. *Validation set-up*

To investigate the analytical expressions for ϵ and δ in more detail and to assess the validity, we use LES of the Dutch Atmospheric LES model (DALES; Cuijpers and Duynkerke, 1993) for three shallow convection cases. Two of the cases are more or less steady state shallow convection cases over tropical oceans designed from the field campaigns BOMEX (Barbados Oceanographic and Meteorological Experiment; Siebesma and Cuijpers, 1995) and RICO (Rain in Tropical Cumulus over the Ocean; Rauber *et al.*, 2007). For RICO we use the 24 h composite run. (More information about this case and the experimental set-up of the composite run can be found online at www.knmi.nl/samenw/rico.) The main differences between these two cases concern the cloud depth ($\sim$ 1000 m for BOMEX and $\sim$ 1700 m for RICO) and

Copyright © 2010 Royal Meteorological Society

the mass flux profiles (more variable in RICO). The third case is based on an idealization of observations made at the Southern Great Plains ARM (Atmospheric Radiation Measurement Program) site on 21 June 1997 (Brown *et al.*, 2002). The ARM case describes the development of daytime shallow cumulus convection over land. After approximately 5 h of simulation, at 1130 LT (local time), clouds start to develop at the top of an initially clear convective boundary layer. From this moment on, the cloud layer grows to a maximum depth of 1500 m at 1630 LT, after which it starts to decrease. Finally, at the end of the day at 1930 LT, all clouds collapse. For the ARM case we solely present results for the cloudy period. Because the ARM case is non-steady, it is pre-eminently suited as a thorough test of our expressions.

For all cases, precipitation is turned off in the LES model (only RICO observations show some light rain) and cloud base level is defined as the height where the mass flux is at its maximum (de Rooy and Siebesma, 2008). For BOMEX and RICO the first hour is excluded for spin-up reasons.

All presented LES results are hourly averaged and based on the cloud core sampling, i.e. all LES gridpoints that contain liquid water and are positively buoyant ($\theta_{v,c} > \overline{\theta_v}$) are considered to be part of the cloudy updraught. Note that recently a sampling method based on passive tracers has been developed (Couvreux *et al.*, 2010) giving comparably good estimates of the total turbulent transport of moist conserved variables in the cloud layer. In principle such a sampling method could be used as an alternative for the core sampling to evaluate the analytical expressions.

Applying the cloud core sampling to determine the updraught properties, the entraining plume model (19) can be used to infer ϵ_{qt} from LES (Siebesma and Cuijpers, 1995). Subsequently, this ϵ_{qt} together with M as diagnosed with the LES cloud core sampling can be substituted in (21) to determine δ (referred to as δ_{qt}). So ϵ_{qt} and δ_{qt} are the lateral mixing coefficients as often diagnosed from LES (Siebesma *et al.*, 2003) and they will be considered here as the reference. Concerning the validation, it is important to mention that δ_{qt} is a function of M which via $M = a_c w_c$ is related to $(1/a_c)\partial a_c/\partial z$ and this term is part of δ_w. Nonetheless, this dependence has no serious impact on the conclusions.

As mentioned by Siebesma *et al.* (2003), the plume model breaks down near the inversion because a simple bulk approach with a single positive entrainment rate is not able to represent the behaviour of the core fields. It is therefore justifiable to exclude the top 15% of the cloudy layer (where the cloud layer is defined as the layer where $a_c > 0$). Also negative ϵ_{qt} and/or δ_{qt} values indicate that the bulk approach breaks down and these situations are therefore excluded from our evaluation. However, when an expression or parametrization of ϵ or δ results in a negative value, it is cut off to zero, as would be done in practice. Note that this cut-off (instead of maintaining the negative value) has no significant impact on the results.

3.2. Results

Before we show the results of the analytical expressions against LES, the sensitivity of Eqs. (27) and (28) for α is investigated. This is done by varying α and showing in Figure 3, for all three investigated cases together, the overall performance of Eqs. (27) and (28) in terms of the RMSE

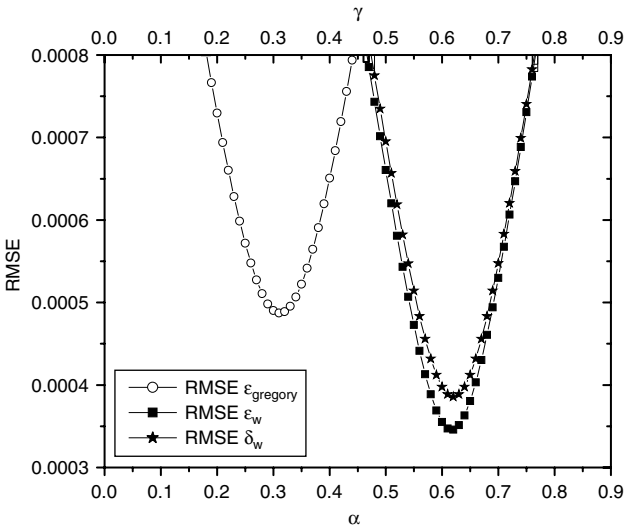

Figure 3. The Root Mean Square Error (RMSE) of $\epsilon_{\text{Gregory}}$ (31) as a function of γ, and ϵ_w (27) and δ_w (28) as functions of α for the ARM, BOMEX and RICO cases together. The RMSE for optimal α (0.62) and γ (0.31) are mentioned in Table I. Note that Gregory (2001) found $\gamma = 12^{-1}$.

defined as

$$RMSE = \sqrt{\frac{1}{N}\sum_{i=1,N}(X_{w,i} - X_{qt,i})^2}\,, \tag{29}$$

where $X \in \{\epsilon, \delta\}$ and i is an index over all presented ($N = 1009$) results. Figure 3 reveals that the optimal α for ϵ_w and δ_w (0.62) coincides and this value is also quite close to the values found by the aforementioned LES experiments (0.6, Voogd, 2009; 0.67, Simpson and Wiggert, 1969). Hereafter all presented results are based on $\alpha = 0.62$.

We start with the non-steady state ARM case, showing in Figures 4(a, b) scatterplots with ϵ_w and δ_w against ϵ_{qt} and δ_{qt}, respectively. Apart from the positive bias for ϵ_w, the correspondence between the analytical expressions and the mixing coefficients as diagnosed from LES is generally good, especially considering the complicated, non-steady-state nature of this case. On the other hand, Figure 4(a) still reveals relatively large overestimations during the beginning (until 1430 LT) and at the last hour (1930 LT) of the cloudy period. Note that at 1930 LT clouds start to collapse and the maximum cloud cover (at cloud base) for this hour is only 0.006, which can be interpreted as an indication that the results for this hour suffer from noise generated by a too small ensemble. In the discussion of the next figures, we will return to the above-mentioned overestimations of the entrainment.

The generally good correspondence of the expressions with the reference lateral mixing coefficients, including the correct height dependence, is confirmed by Figure 5. For clarity reasons, only some selected hours are plotted. Figure 5(a) reveals that the relatively large overestimations in the entrainment at 1330 LT (Figure 4(a)) occur near cloud base. This is also the case for 1230 and 1430 LT (not plotted). However, the aforementioned overestimations of the entrainment at 1930 LT show a much different height dependence with a maximum error at 1800 m, in the middle of the cloud layer (Figure 5(c)). Noteworthy in the detrainment profile plots (Figures 5(b, d)) is the large variation in time. (Note the different x-axis scale for ϵ and

Copyright © 2010 Royal Meteorological Society

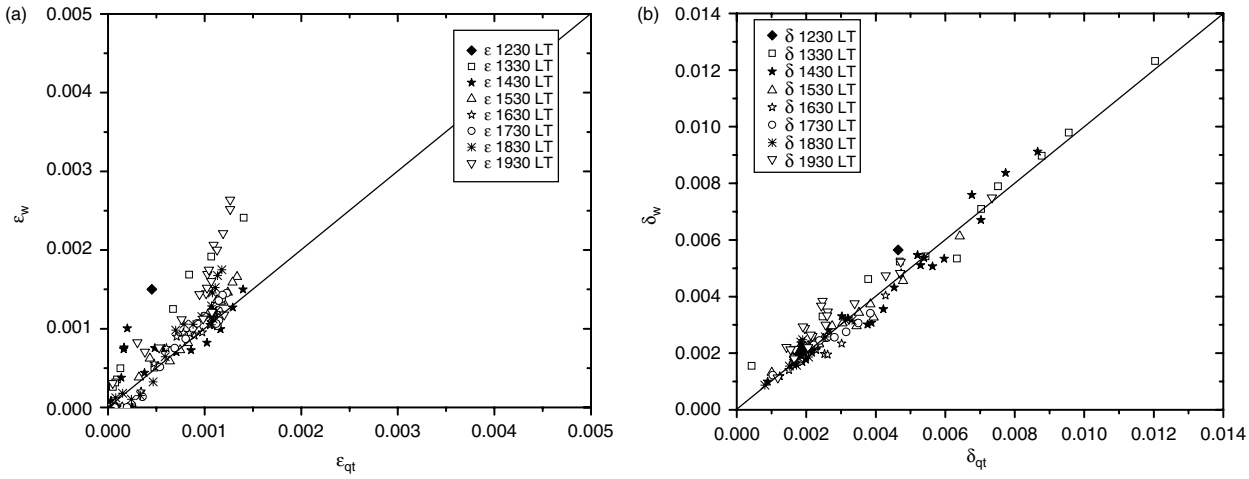

Figure 4. Comparison of (a) ϵ_w with ϵ_{qt} and (b) δ_w with δ_{qt} for different hours during the ARM case.

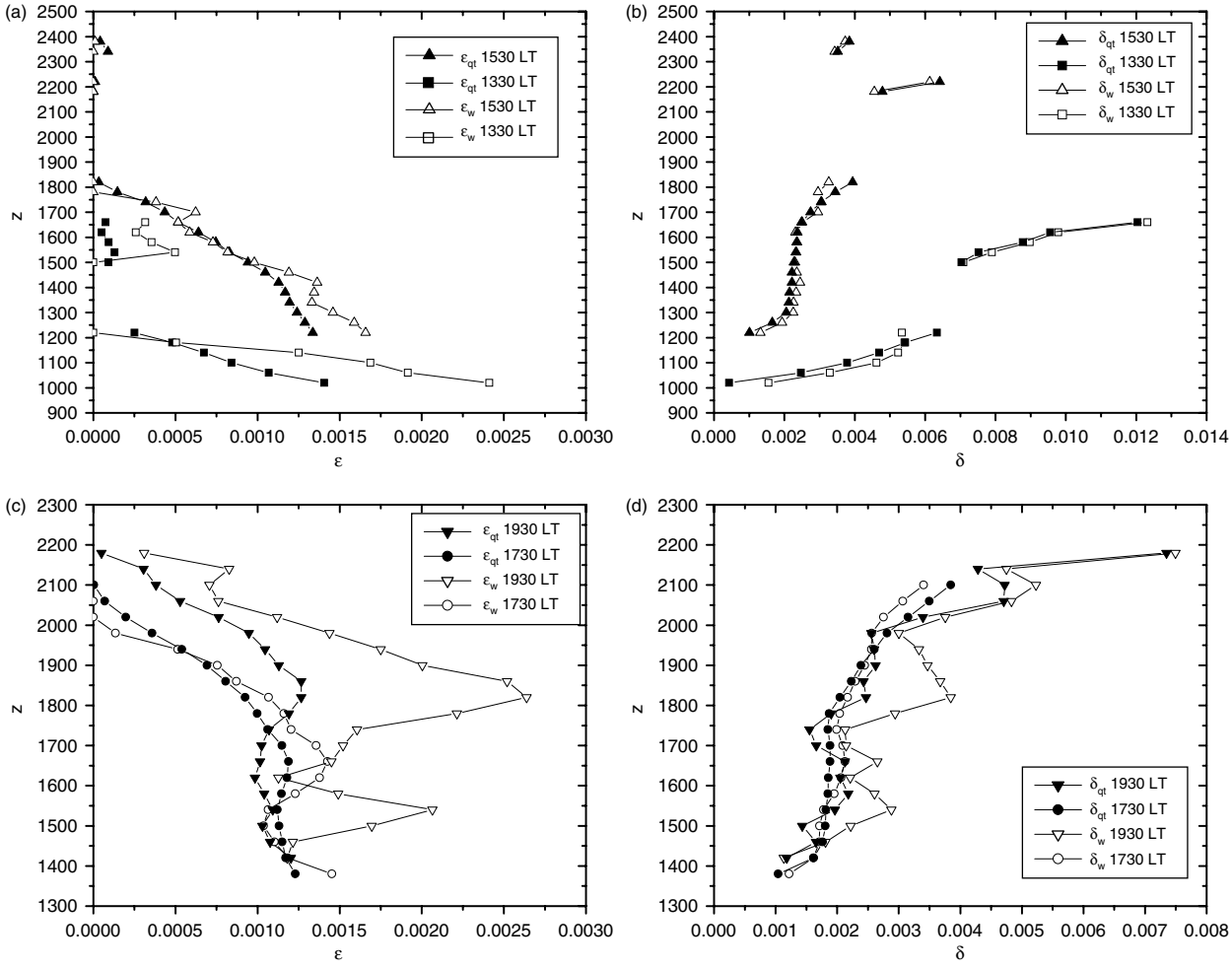

Figure 5. Profiles of ϵ_{qt} (closed symbols) and ϵ_w (open symbols) during the ARM case for hours (a) 1330 and 1530 LT and (c) 1730 and 1930 LT. (b) and (d) are as (a) and (c) but now for δ. Note the different x-axis scale for the entrainment and detrainment plots. Profiles can be discontinuous due to negative ϵ_{qt} and/or δ_{qt} values (see text).

δ.) As explained by de Rooy and Siebesma (2008), the large δ values as observed during the first cloudy hours of the ARM case (Figures 5(b) and 4(b)) are for an important part caused by the relative shallowness of the cloud layers. In a bulk sense (averaged over the cloud layer depth), shallower layers inevitably lead to larger $(1/M)\partial M/\partial z$ and $(1/a_c)\partial a_c/\partial z$ terms ($(1/M)\partial M/\partial z \sim (1/M)\triangle M/\triangle z \sim (1/\triangle z)$). Under the usual divergent conditions, these terms only affect the detrainment ((22) and (28)), explaining the large δ values observed during the first cloudy hours of ARM. Besides the depth of the cloud layer, the shape of the mass flux profile, and therewith δ, is also influenced by environmental conditions (e.g. Derbyshire *et al.*, 2004) as well as properties of the updraught itself (de Rooy and Siebesma, 2008). The above-mentioned arguments support the approach of de Rooy and Siebesma (2008) to describe

Copyright © 2010 Royal Meteorological Society

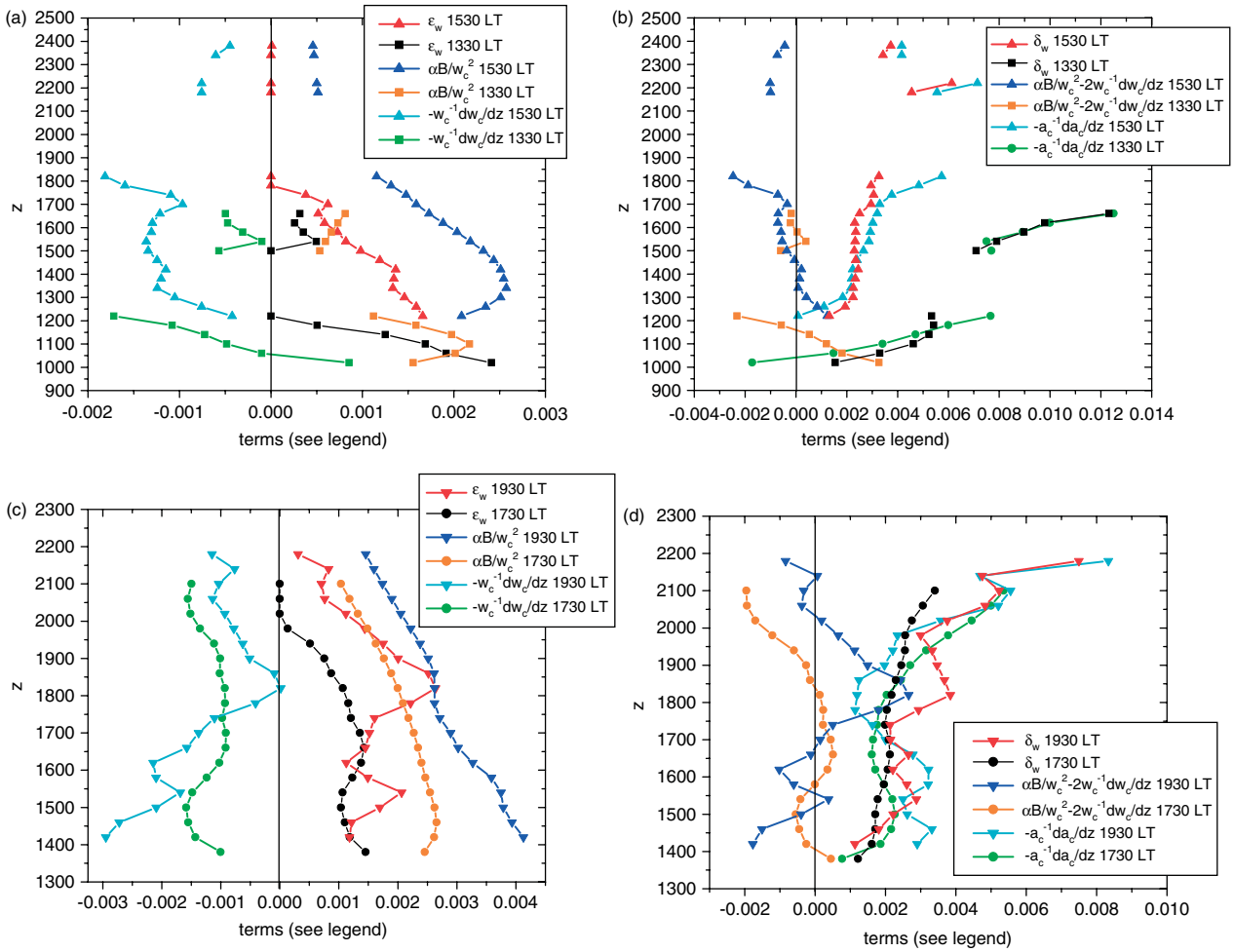

Figure 6. For different hours during the ARM case, profiles of (a, c) ϵ_w and (b, d) δ_w including the terms which build up the corresponding expressions, that is $(\alpha B w_c^{-2})$ and $(-w_c^{-1}\partial w_c/\partial z)$ for ϵ_w, and $(\alpha B w_c^{-2} - 2w_c^{-1}\partial w_c/\partial z)$ and $(-a_c^{-1}\partial a_c/\partial z)$ for δ_w (with $\alpha = 0.62$).

the mass flux profile with a fixed function for ϵ but a flexible parametrization for δ to account for the variations in the shape from hour to hour and case to case (e.g. a strong or zero decrease of the mass flux in the lowest half of the cloud layer). An interesting variation on this approach is given by Neggers *et al.* (2009) describing changes in the cloud fraction profile based on thermodynamical arguments.

Now, again for the ARM case only, let us take a closer look at the different terms building up the expressions for ϵ and δ and their impact on the vertical profiles of ϵ_w and δ_w (Figures 6(a–d), again for the selected hours as in Figure 5). We first return to the relatively large overestimations of the entrainment during the first cloudy hours and 1930 LT mentioned before. Comparing Figures 5(a) and (c) with Figures 6(a) and (c) reveals that the large overestimations in ϵ are related to conditions with positive (or small negative) $-(1/w_c)\partial w_c/\partial z$ values. Also for 1230 and 1430 LT (not plotted) the largest overestimations in the entrainment occur when $-(1/w_c)\partial w_c/\partial z > 0$ (i.e. w_c decreases with height). The $-(1/w_c)\partial w_c/\partial z$ profile for 1930 LT (Figure 6(c)) is quite different from all other hours with a positive value in the middle of the cloud layer at 1800 m (also the height with the maximum error in ϵ_w and δ_w for this hour) and a decrease above. This atypical profile supports the aforementioned suspicion that the ensemble for this hour is too small.

The overall picture of Figures 6(a) and (c) is that both terms in (27) for ϵ_w, i.e. $\alpha B/w_c^2$ and $(1/w_c)\partial w_c/\partial z$, are of the same order of magnitude, with the buoyancy term being somewhat larger. However, for δ_w (Figures 6(b) and (d)) the situation is different. Because the sum of the buoyancy and the vertical velocity terms in (28) for δ_w, i.e.

$$\frac{\alpha B}{w_c^2} - \frac{2}{w_c}\frac{\partial w_c}{\partial z},$$

result mostly in small negative values for a large part of the cloud layer, the strongly fluctuating $(1/a_c)\partial a_c/\partial z$ term clearly dominates the height and time variation in δ. As a result, δ_w can be reasonably well approximated by $-(1/a_c)\partial a_c/\partial z$ with generally underestimations near cloud base and overestimations near cloud top. Also a direct comparison between δ_{qt} and $-(1/a_c)\partial a_c/\partial z$ for all three cases together gives reasonable results (Figure 7(a)).

If we assume that δ can be approximated by $-(1/a_c)\partial a_c/\partial z$, this leads together with (21) to the formulation proposed by Nordeng (1994):

$$\epsilon_{\text{Nordeng}} = \frac{1}{w_c}\frac{\partial w_c}{\partial z}. \tag{30}$$

However, from Figure 7(b) it becomes clear that, although the aforementioned approximation works well for δ, it does not hold for ϵ where the equal order of magnitude of the different terms in the analytical expression makes this

Copyright © 2010 Royal Meteorological Society

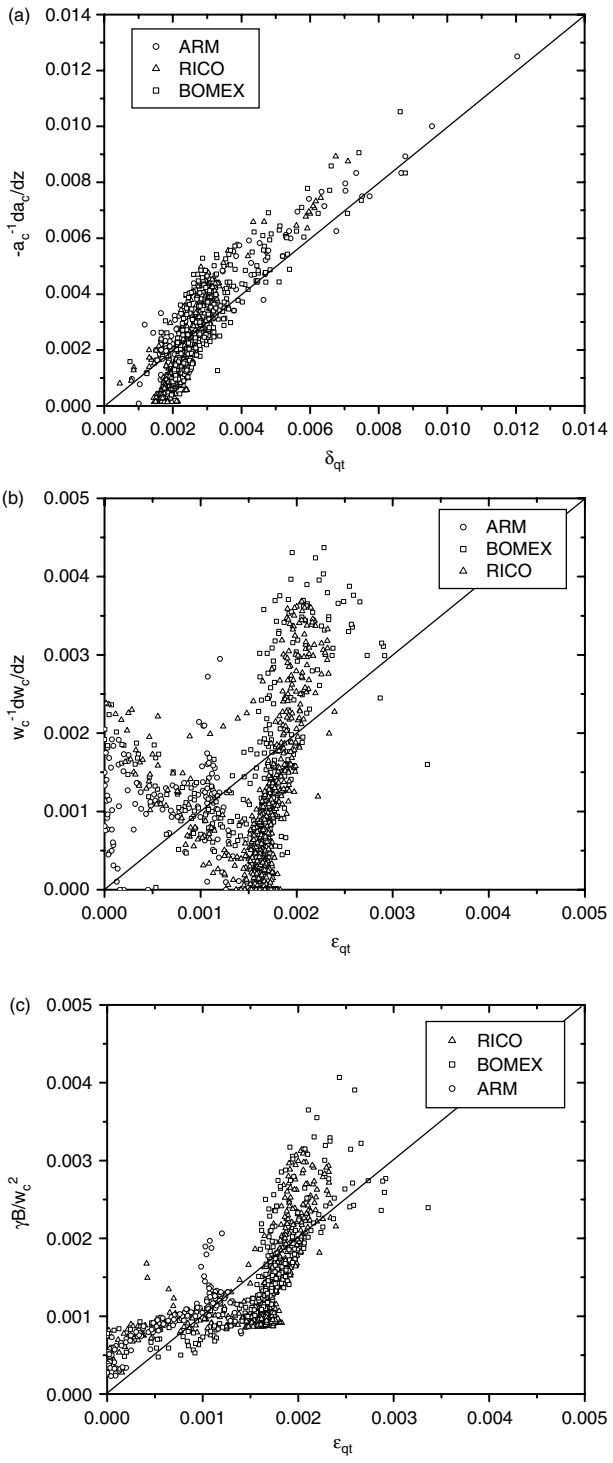

Figure 7. For the ARM, BOMEX, and RICO cases, comparison of (a) δ_{qt} with $-1(1/a_c)\partial a_c/\partial z$, (b) ϵ_{qt} with $\epsilon_{\text{Nordeng}} = w_c^{-1}\partial w_c/\partial z$, and (c) ϵ_{qt} with $\epsilon_{\text{Gregory}} = \gamma B w_c^{-2}$, with $\gamma = 0.31$.

expression more sensitive. From an overestimation of high values of ϵ_{qt} in Figure 7(b), corresponding to values near cloud base, (30) underestimates ϵ values in the middle of the cloud layer and again overestimates the small ϵ values near the top of the cloud layer. For all three cases together, the RMSE for (30) is presented in Table I.

Yet another approximation can be made by simply ignoring the $(1/w_c)\partial w_c/\partial z$ term (Figure 6(a) and (c)) in (27), leading to the following expression, as proposed by Gregory (2001)

$$\epsilon_{\text{Gregory}} = \frac{\gamma B}{w_c^2}, \tag{31}$$

where γ represents a tuning constant. Gregory (2001) used $\gamma = 1/12$ and found a 50% underestimation of his expression against LES for BOMEX. The sensitivity of (31) for γ is shown in Figure 3 which suggests a much higher optimal value, namely $\gamma = 0.31$. To demonstate the potential of (31), we show results with the latter optimal value. Figure 7(c) for all three cases reveals reasonable results for (31) but less good than with the full analytical expression 27 (compare Figure 7(c) with Figures 4(a) and 8(a) or see Table I or Figure 3). Especially for BOMEX and RICO, the $(1/w_c)\partial w_c/\partial z$ term (not shown) has relatively large values near cloud base and cloud top. Consequently, $\epsilon_{\text{Gregory}}$ in Figure 7(c) reveals inevitably a bend in the scatterplot with overestimations near cloud base and top and underestimations around the middle of the cloud layer. Another indication that the influence of $(1/w_c)\partial w_c/\partial z$ cannot be ignored in an expression for ϵ comes from examining the profiles in Figure 5(c) in detail. For example, looking just above 1500 m for 1730 LT, ϵ atypically increases slightly with height. This increase is caused by the increase of $-(1/w_c)\partial w_c/\partial z$ at the corresponding height (Figure 6(c)). Although such increases in ϵ_w are generally at the approximately correct heights, they seem to be somewhat stronger than in ϵ_{qt}, especially for hour 1930 LT. As well as Gregory, Mironov (2009) and Rio *et al.* (2010) also mentioned the term B/w_c^2 in an expression for the lateral mixing coefficients.

As a validity check we also present results for the steady state cases BOMEX and RICO (Figure 8). Again the correspondence between the usual LES diagnosed mixing coefficients and ϵ_w and δ_w is good. While the analytical expressions overestimated the entrainment for ARM, they seem to underestimate the detrainment for BOMEX and RICO somewhat. The RMSE for the analytical expressions 27 and 28 for all cases together are presented in Table I.

In comparison with δ, the variations from hour to hour and case to case in ϵ are small (Figure 5) and describing ϵ with some fixed (non-dimensionalized) function from cloud base to cloud layer top seems more feasible than a fixed function for δ (also de Rooy and Siebesma, 2008). But despite the relative small variation in ϵ profiles, the results clearly show overall smaller entrainment rates for the ARM case than for the BOMEX and RICO case (compare Figure 4(a) with Figure 8). This is caused by the smaller $\alpha B/w_c^2$ term, and more specifically the larger

Table I. Root Mean Square Error of different expressions for ϵ and δ against ϵ_{qt} and δ_{qt} respectively for the ARM, BOMEX and RICO case together (N=1009). Results for ϵ_w and δ_w are based on $\alpha = 0.62$ and for $\epsilon_{\text{Gregory}}$ on $\gamma = 0.31$.

	RMSE
ϵ_w	3.45×10^{-4}
$\epsilon_{\text{Gregory}}$	4.87×10^{-4}
$\epsilon_{\text{Nordeng}}$	1.01×10^{-3}
δ_w	3.85×10^{-4}

Copyright © 2010 Royal Meteorological Society

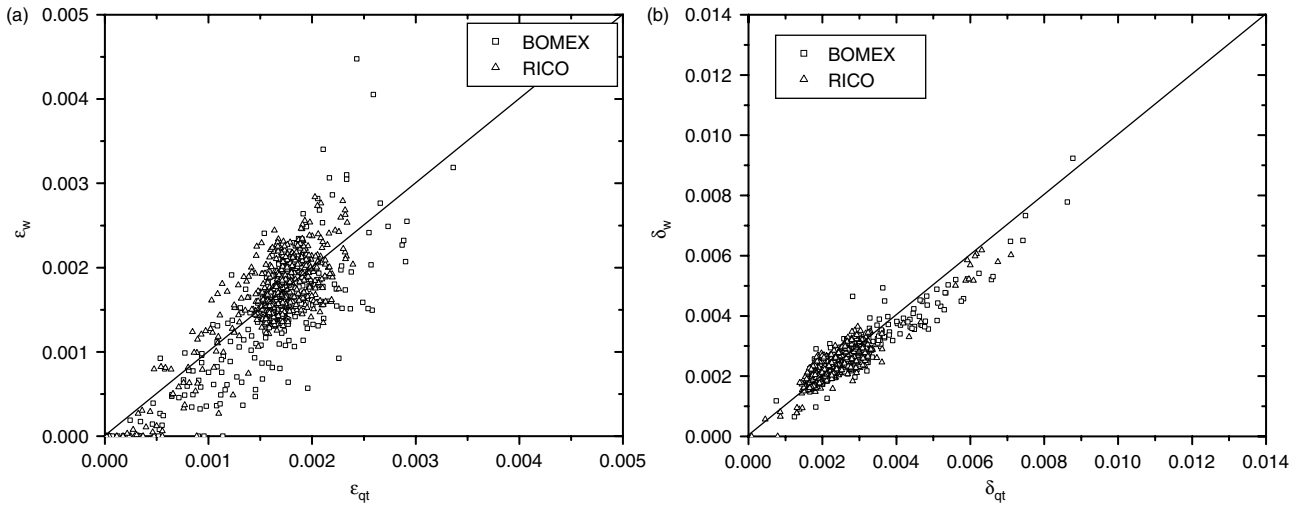

Figure 8. Comparison of (a) ϵ_{qt} with ϵ_w and (b) δ_{qt} with δ_w, for all hours except the first during the BOMEX and RICO cases.

vertical velocity in the ARM case. For example, at cloud base $w_c \approx 1.5\,\mathrm{m\,s^{-1}}$ for ARM whereas $w_c \approx 0.7\,\mathrm{m\,s^{-1}}$ for BOMEX and RICO. The higher velocities during the ARM case can be related to the more vigorous convection in the subcloud layer with strong surface heating above land. If we are able to make an adequate estimate of the vertical velocity of the updraught at cloud base in a NWP or climate model, this velocity can be used to refine the often-applied parametrization where ϵ is a fixed function of height (e.g. Siebesma *et al.*, 2003), i.e. parametrize the starting value of ϵ at cloud base with a function of the vertical velocity of the updraught and assume e.g. a z^{-1} lapse rate for the rest of the cloud layer. This is an example of how insight given by the analytical expressions can be used for parametrization developments. Note that the ARM case has a much deeper subcloud layer than the other two cases, enabling not only larger accelerations of the updraught thermals but also the development of larger thermals that will normally have smaller ϵ values. A separation between these positively correlated updraught properties, high updraught vertical velocity and large sizes of the thermals, cannot be made here.

4. Conclusions and discussion

In contrast with other studies on fractional entrainment and detrainment (e.g. Gregory, 2001; Siebesma *et al.*, 2003), where the development of parametrizations was the main goal, here we primarily wanted to gain more insight into the behaviour and physical nature of ϵ and δ. For that, we derived analytical expressions for ϵ and δ starting from generally valid equations for arbitrary-shaped in-cloud fields and subsequently applied assumptions known from literature. In contrast with most other theoretical studies on convection, we did not assume a constant cloudy area fraction with height which is crucial because we consider an ensemble of updraughts for which it is known that the cloudy area fraction can vary strongly with height. One of the key assumptions in the derivation concerns the description of the fluxes across the cloudy boundaries, where we follow Asai and Kasahara (1967) including the distinction between larger-scale dynamical transport and small-scale turbulent mixing.

From the derivation of the analytical expressions, the following physical picture (Figure 2) emerges for an ensemble of shallow cumulus clouds under the usual divergent situation ($\partial M/\partial z < 0$): Massive entrainment occurs just beneath cloud base (here defined as the level with maximum mass flux). From cloud base to cloud top, individual clouds have a constant mass flux with only turbulent lateral mixing until the massive detrainment at the cloud top. This picture is in line with Arakawa and Schubert (1974) and Nordeng (1994), but now includes a turbulent detrainment term. As a result of different cloud sizes in the ensemble, the massive detrainment of the various clouds shows up as a dynamical detrainment term and the overall mass flux decreases with height. The consequence of the above-mentioned concept is that, in the cloud layer, ϵ is only determined by turbulent lateral mixing whereas δ is also influenced by dynamical transport ($(1/M)\partial M/\partial z$). As a result there is a strong correspondence between variations in δ and $(1/M)\partial M/\partial z$ (or $(1/a_c)\partial a_c/\partial z$), which supports the approach of de Rooy and Siebesma (2008) to describe the mass flux profile with a fixed function for ϵ but a flexible parametrization of δ to account for the often described substantial variations in the shape. For example, from de Rooy and Siebesma (2008), we know that δ varies strongly with cloud layer depth. This can now be easily explained because in a bulk sense (averaged over the cloud layer) and under (the usual) divergent conditions, $(1/M)\partial M/\partial z$ and $(1/a_c)\partial a_c/\partial z$, and therewith δ, must increase with decreasing cloud layer depth.

Based on a continuity equation and budget equations for the updraught vertical velocity and total water specific humidity, analytical expressions for ϵ and δ are derived. The first term in the expressions, $\alpha B/w_c^2$, is similar to the expression for ϵ as proposed by Gregory (2001). Further, it is shown that under certain assumptions both terms in the expression for ϵ together can be written as the expression suggested by Nordeng (1994). Overall, results with $\epsilon_{\mathrm{Gregory}}$ and especially $\epsilon_{\mathrm{Nordeng}}$ are less accurate than the analytical expression ϵ_w. Moreover, with the help of the full expression, biases in $\epsilon_{\mathrm{Gregory}}$ and $\epsilon_{\mathrm{Nordeng}}$ can be explained.

Although the variations from case to case and hour to hour in ϵ are smaller than in δ, the entrainment values diagnosed for the ARM case are significantly smaller than for the BOMEX and RICO case. The analytical expression

Copyright © 2010 Royal Meteorological Society

for ϵ reveals that this difference can be related to the much smaller B/w_c^2 term, or more specifically much larger w_c values, in the ARM case. It is discussed how this insight given by the analytical expression for ϵ can be useful for the development of a new parametrization.

Although we used assumptions already known from literature in the derivation of the expressions, this does not mean that all applied assumptions were straightforward and undisputed. A problematic point remains the determination of a proper value for the buoyancy reduction factor α which covers the subplume turbulence term of the vertical velocity variance as well as the pressure perturbation term. In principle, α should be objectively derived from a careful analysis of the vertical velocity budget terms in LES. But even then it is not yet established if α can be considered as approximately constant under all conditions. For example, Holton (1973) already pointed out that the importance of the pressure perturbation term will increase going from shallow to deep heavy precipitating convection. Nevertheless, preliminary results from LES experiments diagnosing the vertical velocity budget terms (Voogd, 2009), early results based on water tank experiments (Turner, 1963; Simpson and Wiggert, 1969), as well as the results presented here, all suggest a suitable value for α of around 0.62 for shallow convective conditions.

The presented analytical expressions are useful to identify important processes determining the behaviour of ϵ and δ. It is shown that the expressions can be used as a starting point for the development of parametrization approaches as well as to judge existing parmetrizations.

Acknowledgements

Three anonymous reviewers are thanked for their useful comments. Pier Siebesma acknowledges fruitful discussions in an early stage of this research with David Neelin and Harm Jonker. This study has benefited from meetings funded by COST ES0905.

References

Arakawa A, Schubert WH. 1974. Interaction of a cumulus cloud ensemble with the large-scale environment, Part I. *J. Atmos. Sci.* **31**: 674–701.

Asai T, Kasahara A. 1967. A theoretical study of the compensating downward motions associated with cumulus clouds. *J. Atmos. Sci.* **24**: 487–496.

Bechtold P, Köhler M, Jung T, Doblas-Reyes F, Leutbecher M, Rodwell M, Vitart F, Balsamo G. 2008. Advances in simulating atmospheric variability with the ECMWF model: From synoptic to decadal time-scales. *Q. J. R. Meteorol. Soc.* **134**: 1337–1351.

Betts AK. 1975. Parametric interpretation of trade-wind cumulus budget studies. *J. Atmos. Sci.* **32**: 1934–1945.

Bretherton CS, McCaa JR, Grenier H. 2004. A new parameterization for shallow cumulus convectionn and its application to marine subtropical cloud-topped boundary layers. Part I: Description and 1D results. *Mon. Weather Rev.* **132**: 864–882.

Brown AR, Cederwall RT, Chlond A, Duynkerke PG, Golaz J-C, Khairoutdinov J, Khairoutdinov M, Lewellen DC, Lock AP, Macvean MK, Moeng C-H, Neggers RAJ, Siebesma AP, Stevens B. 2002. Large-eddy simulation of the diurnal cycle of shallow cumulus convection over land. *Q. J. R. Meteorol. Soc.* **128**: 1075–1094.

Cotton WR. 1975. On parameterization of turbulent transport in cumulus clouds. *J. Atmos. Sci.* **32**: 548–564.

Couvreux F, Hourdin F, Rio C. 2010. Resolved versus parameterized boundary-layer plumes. Part I: A parameterization-oriented conditional sampling in large-eddy simulations. *Boundary-Layer Meteorol.* **134**: 441–458.

Cuijpers JWM, Duynkerke PG. 1993. Large-eddy simulation of trade-wind cumulus clouds. *J. Atmos. Sci.* **50**: 3894–3908.

de Rooy WC, Siebesma AP. 2008. A simple parameterization for detrainment in shallow cumulus. *Mon. Weather Rev.* **136**: 560–576.

Derbyshire SH, Beau I, Bechtold P, Grandpeix J-Y, Piriou J-M, Redelsperger J-L, Soares PMM. 2004. Sensitivity of moist convection to environmental humidity. *Q. J. R. Meteorol. Soc.* **130**: 3055–3079.

Grant ALM, Brown AR. 1999. A simililarity hypothesis for shallow cumulus transports. *Q. J. R. Meteorol. Soc.* **125**: 1913–1936.

Gregory D. 2001. Estimation of entrainment rate in simple models of convective clouds. *Q. J. R. Meteorol. Soc.* **127**: 53–72.

Gregory D, Rowntree PR. 1990. A mass flux convection scheme with representation of cloud ensemble characteristics and stability-dependent closure. *Mon. Weather Rev.* **118**: 1483–1506.

Gregory D, Morcrette J-J, Jakob C, Beljaars ACM, Stockdale T. 2000. Revision of convection, radiation and cloud schemes in the ECMWF Integrated Forecasting System. *Q. J. R. Meteorol. Soc.* **126**: 1685–1710.

Holloway CE, Neelin JD. 2009. Moisture vertical structure, column water vapor, and tropical deep convection. *J. Atmos. Sci.* **66**: 1665–1683.

Holton JR. 1973. A one-dimensional cumulus model including pressure perturbations. *Mon. Weather Rev.* **101**: 201–205.

Houghton H, Cramer H. 1951. A theory of entrainment in convective currents. *J. Meteorol.* **8**: 95–102.

Kain JS, Fritsch JM. 1990. A one-dimensional entraining/detraining plume model and its application in convective parameterization. *J. Atmos. Sci.* **47**: 2784–2802.

Kuo HL. 1962. On the controlling influences of eddy diffusion on thermal convection. *J. Atmos. Sci.* **19**: 236–243.

Lappen C-L, Randall DA. 2001. Toward a unified parameterization of the boundary layer and moist convection. Part II: Lateral mass exchanges and subplume-scale fluxes. *J. Atmos. Sci.* **58**: 2037–2051.

List R, Lozowski EP. 1970. Pressure pertubations and buoyancy in convective clouds. *J. Atmos. Sci.* **27**: 168–170.

Mironov DV. 2009. Turbulence in the lower troposphere: Second-order closure and mass-flux modelling frameworks. In *Interdisciplinary aspects of turbulence*. Springer-Verlag: Berlin. 161–221.

Morton BR, Taylor GI, Turner JS. 1956. Turbulent gravitational convection from maintained and instantaneous sources. *Proc. R. Soc. London A* **234**: 1–23.

Murphy JM, Sexton DMH, Barnett DN, Jones GS, Webb MJ, Collins M, Stainforth DA. 2004. Quantification of modelling uncertainties in a large ensemble of climate change simulations. *Nature* **430**: 768–772.

Neggers RAJ, Siebesma AP, Jonker HJJ. 2002. A multiparcel method for shallow cumulus convection. *J. Atmos. Sci.* **59**: 1655–1668.

Neggers RAJ, Köhler M, Beljaars ACM. 2009. A dual mass flux framework for boundary-layer convection. Part I: Transport. *J. Atmos. Sci.* **66**: 1464–1487.

Nordeng TE. 1994. *'Extended versions of the convective parameterization scheme at ECMWF and their impact on the mean and transient activity of the model in the Tropics'*. Technical Memo. No. 206, ECMWF: Reading, UK.

Randall DA, Huffman GJ. 1982. Entrainment and detrainment in a simple cumulus cloud model. *J. Atmos. Sci.* **39**: 2793–2806.

Rauber RM, Ochs, III HT, Di Girolamo L, Göke S, Snodgrass E, Stevens B, Knight C, Jensen JB, Lenschow DH, Rilling RA, Rogers DC, Stith JL, Albrecht BA, Zuidema P, Blyth AM, Fairall CW, Brewer WA, Tucker S, Lasher-Trapp SG, Mayol-Bracero OL, Vali G, Geerts B, Anderson JR, Baker BA, Lawson RP, Bandy AR, Thornton DC, Burnet E, Brenguier J-L, Gomes L, Brown PRA, Chuang P, Cotton WR, Gerber H, Heikes BG, Hudson JG, Kollias P, Krueger SK, Nuijens L, O'Sullivan DW, Siebesma AP, Twohy CH. 2007. Rain in Shallow Cumulus Over the Ocean: The RICO Campaign. *Bull. Amer. Meteorol. Soc.* **88**: 1912–1928.

Raymond DJ, Blyth AM. 1986. A stochastic mixing model for non-precipitating cumulus clouds. *J. Atmos. Sci.* **43**: 2708–2718.

Rio C, Hourdin F, Couvreux F, Jam A. 2010. Resolved versus parameterized boundary-layer plumes. Part II: Continuous formulations of mixing rates for mass-flux schemes. *Boundary-Layer Meteorol.* In press.

Rougier J, Sexton DMH, Murphy JM, Stainforth D. 2009. Analyzing the climate sensitivity of the HadSM3 climate model using ensembles from different but related experiments. *J. Climate* **22**: 3540–3557.

Siebesma AP. 1998. Shallow cumulus convection. In *Buoyant Convection in Geophysical Flows*, Plate EJ, Fedorovich EE, Viegas XV, Wyngaard JC. (eds.) **513**: Kluwer Academic Publishers: 441–486.

Siebesma AP, Cuijpers JWM. 1995. Evaluation of parametric assumptions for shallow cumulus convection. *J. Atmos. Sci.* **52**: 650–666.

Siebesma AP, Bretherton CS, Brown A, Chlond A, Cuxart J, Duynkerke PG, Jiang H, Khairoutdinov M, Lewellen D, Moeng C-H, Sanchez E, Stevens B, Stevens DE. 2003. A large-eddy simulation intercomparison study of shallow cumulus convection. *J. Atmos. Sci.* **60**: 1201–1219.

Copyright © 2010 Royal Meteorological Society

Simpson J, Wiggert V. 1969. Models of precipitating cumulus towers. *Mon. Weather Rev.* **97**: 471–489.
Stevens B, Ackerman AS, Albrecht BA, Brown AR, Chlond A, Cuxart J, Duynkerke PG, Lewellen DC, Macvean MK, Neggers RAJ, Sanchez E, Siebesma AP, Stevens DE. 2001. Simulations of trade-wind cumuli under a strong inversion. *J. Atmos. Sci.* **58**: 1870–1891.
Stommel H. 1947. Entrainment of air into a cumulus cloud. *J. Meteorol.* **4**: 91–94.
Tiedtke M. 1989. A comprehensive mass flux scheme for cumulus parameterization in large-scale models. *Mon. Weather Rev.* **177**: 1779–1800.
Turner JS. 1963. The motion of buoyant elements in turbulent surroundings. *J. Fluid Mech.* **16**: 1–16.
Voogd Y. 2009. 'Parameterization of the vertical velocity in shallow cumulus clouds'. Bachelor thesis, Department of Multi-scale Physics, Delft University of Technology, The Netherlands.
Warner J. 1955. The water content of cumuliform clouds. *Tellus* **7**: 449–457.

Copyright © 2010 Royal Meteorological Society